



Custom-built light-pipe cell for high-resolution infrared absorption spectroscopy of tritiated water vapor and other hazardous gases

JOHANNES MÜLLER,¹ MAGNUS SCHLÖSSER,^{1,*} FRANK HASE,²
NICOLAS ZIEGLER,¹ ROBIN GRÖSSLE,¹ DAVID HILLESHEIMER,¹ AND
JOHANNES ORPHAL²

¹Tritium Laboratory Karlsruhe (TLK), Institute for Nuclear Physics (IKP), Karlsruhe Institute of Technology (KIT), P. O. Box 3640, 76021 Karlsruhe, Germany

²Institute of Meteorology and Climate Research (IMK-ASF), Karlsruhe Institute of Technology (KIT), P. O. Box 3640, 76021 Karlsruhe, Germany

*magnus.schloesser@kit.edu

Abstract: We present a new custom-built cell for high-resolution absorption spectroscopy of hazardous gases. The use of an aluminum light-pipe enables sensitive detection due to the small tube diameter and an increased particle density in the interaction volume for a limited analyte amount in the cell, while avoiding additional surfaces such as mirrors. To demonstrate this, we have used the cell to measure tritiated water isotopologues (HTO and traces of T₂O) for which spectroscopic data is scarce, due to the challenge of performing spectroscopy of these highly radio-chemical aggressive substances. For this purpose, the new cell also features the efficient inline-production of tritiated water. In this paper we present the concept of the light-pipe cell and demonstrate its performance with a high-resolution absorption spectrum of gaseous HTO generated inside of this cell.

© 2019 Optical Society of America under the terms of the [OSA Open Access Publishing Agreement](#)

1. Introduction

High resolution spectroscopy is a powerful tool to understand molecular structure and dynamics, as well as for the detection of gases even in very small amounts, e.g. in the Earth's atmosphere, in the interstellar medium, or in combustion and industrial environments. For this, highly accurate spectroscopic reference measurements in the laboratory are indispensable. However, when spectroscopy of hazardous gases is performed in the laboratory, special requirements become relevant with regard to safe handling and processing of the samples. For example, the target species may be dangerous for the health of the analyst in case of exposure (carcinogen, toxic, or radioactive) or it may be aggressive towards the materials of the confining spectroscopy cell. Furthermore, it may only be available or allowed up to a certain maximum sample amount, or it needs to be generated inside of the spectroscopy cell. In this work, we present a new small light-pipe cell to tackle these challenges, and illustrate its performance by high-resolution absorption spectroscopy of tritiated water vapour.

Spectroscopy of tritiated water is of great interest for molecular physics [1–3], but also for the safety of thermonuclear fission (e.g. [4]) or fusion reactors (e.g. [5–7]), and for theoretical calculations of fusion fuel cycle process optimization.

Approaches to use gas-phase infrared absorption spectroscopy with laser-based setups for tritiated water detection in the gas phase have been pursued by Cherrier and Reid [8], Kobayashi et al. [9] and Bray et al. [10] in the past. These techniques offer in general sufficient signal-to-noise ratios for trace detection, but are technically limited in the spectral tuning range of the photon source. Fourier-transform infrared spectroscopy (FTIR) is the method of choice when one aims to perform spectroscopy over wide spectral regions at high spectral resolution. Starting in 1984,

high-resolution FTIR spectroscopy of tritiated water was performed for a few selected bands and isotopologues ($T_2^{16}O$, $HT^{16}O$, $T_2^{18}O$) as reported by Fry et al. [11], Kanesaka et al. [12], and Cope et al. [13, 14].

However, high-resolution spectroscopic data on tritiated water species is still rather limited as documented above. The development of monitoring devices for nuclear applications and the progress of quantum-chemical theory of the water molecule within a large mass range, requires to revive the effort on the spectroscopy of these experimentally challenging isotopologues. For this purpose, our goal is to study radioactive tritiated water samples using high-resolution FTIR spectroscopy. The samples are measured in a FTIR system which is located outside of a licensed laboratory. This limits to an activity of 1 GBq ($\sim 4.6 \cdot 10^{-7}$ mol) - the legal limit for tritium according to German law.

This paper discusses the methodology and technical realization of a spectroscopic cell which enables the in-situ production of tritiated water together with a highly sensitive technique for achieving a maximal signal-to-noise ratio at a limited sample amount. We demonstrate the performance of the cell with regard to tritiated water sample generation and to spectroscopy. Note that many technical aspects of this cell are interesting also for other applications concerning the spectroscopy of hazardous species.

2. Design of a tritium compatible infrared cell

The goal of building a tritium compatible cell which can be coupled to a high-resolution FTIR spectrometer is to strongly extend the sparse spectroscopic data available for tritiated water molecules. Fig. 1 (top) shows a theoretical prediction of the spectrum the $HT^{16}O$ molecule. The spectrum is composed of many vibrational modes (ν_1 , ν_2 , ν_3 and overtones) with high-resolution rotational substructure that can be used, e.g. for detection of HTO. The figure shows which branches have been observed previously by broadband FTIR studies and regions that have been studied using laser spectrometers (which generally cover only a few tens of wavenumbers). This example shows that there are many unobserved bands. The situation is similar for T_2O . For other isotopologues such as DTO or tritiated water molecules containing O-17 or O-18, hardly any data can be found in the literature.

Therefore, our goal was to conceive an experimental method which is suitable to produce a tritiated water sample in a controlled manner and to couple it to a high resolution FTIR-spectrometer, while fulfilling all tritium-related safety requirements.

2.1. Requirements

Tritiated water is strongly radiochemically active as it produces molecular, ionic and radical components originating from the beta-decay [20]. These highly reactive components can evoke secondary reactions if hydrocarbons are present in the vicinity. Especially, halogen containing components need to be avoided as their radiation-induced decomposition can lead to halogen hydrides (e.g. TF, TCl, ...). Thus, in order to protect the tritiated sample from generation of impurities as well as the structural materials (e.g. walls, windows and seals) from loss of integrity, it is a requirement to produce a cell which is free of plastics, rubber, oil and similar organic materials. Most recommended are i) metals like stainless steel, aluminum, gold or copper, ii) ceramics, and iii) glasses.

Besides of proper selection of materials, it is required that the tritium-bearing devices fulfill certain rules which enable safe enclosure of the tritium. This includes that the leak rate of every welding or fitting connection is better than 10^{-9} mbar ℓs^{-1} and an integral leak rate of better than 10^{-8} mbar ℓs^{-1} .

In general, laboratories which routinely operate high-resolution spectrometers do not possess a license for the use of tritium. The legal limit for using tritium without special licensing is 1 GBq as defined by the German Radiation Protection Ordinance as of 2018. It should be noted,

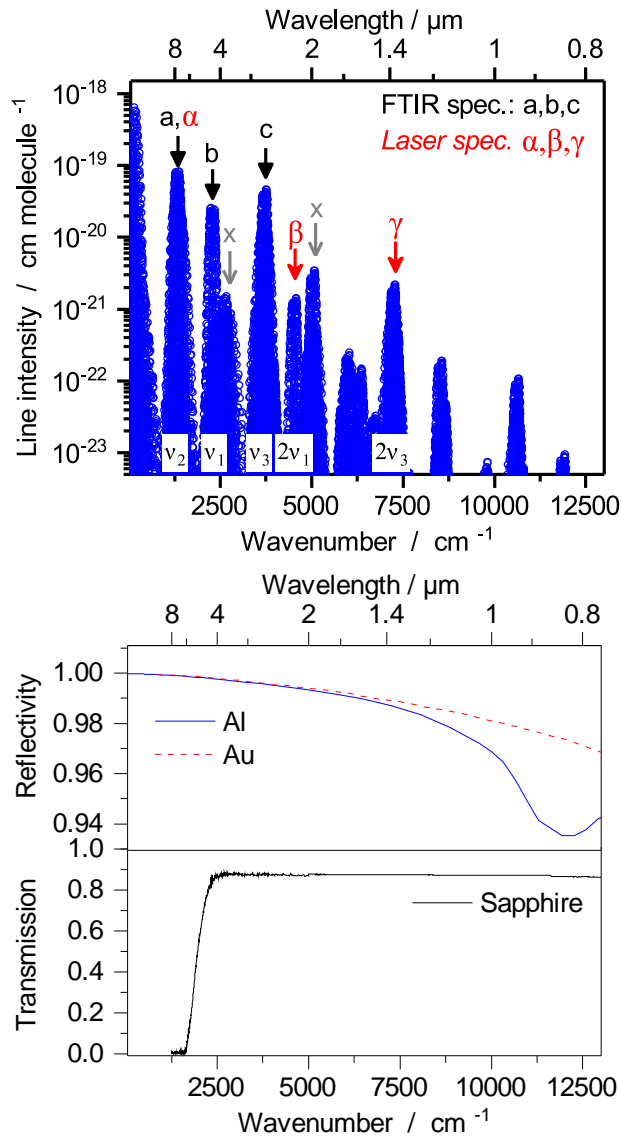


Fig. 1. (Top) Ro-vibrational spectrum of the HT^{16}O molecule. The line positions and intensities are adopted from the Tomsk variational calculation database (<http://spectra.iao.ru/>). Existing spectroscopic studies of different rovibrational bands are indicated. FTIR studies: a) Ulenikov [15], b) Cope [14], c) Fayt [16]. Laser spectrometer studies: α) Cherrier [8], β) Bray [10], γ) Down [17]. The x symbol indicates bands which can be observed by high-resolution FTIR. (Bottom) Reflectivity of our new light-pipe cell material aluminum [18] (and gold [19]) and the transmission through sapphire (from Thorlabs Inc.) in the wavelength range relevant for FTIR studies of tritiated water isotopologues.

that following the European Council Directive 2013/59/EURATOM this value applies in all states of the European Union. For countries outside of the EU other limits may be binding. This is equivalent to an amount of $4.6 \cdot 10^{-7}$ mol of T_2 , considering the half-life of tritium ($t_{1/2} = 4497 \pm 4$ d [21]). At room temperature, this yields a value of $pV = 11$ mbar cm^3 for any gas with two tritium atoms (like T_2 , T_2O , NT_2H , ...).

So, as the sample amount is limited, enhancement of the absorption is required in order to obtain a strong signal-to-noise ratio. Typical enhancement methods are internal multi-reflection cells or cavity-enhanced techniques (see e.g. [22, 23]).

The cell should be either reusable in order to optimize the scientific output by the possibility of exchanging the sample, or, if this is not possible, then the cell materials and manufacturing cost should be low when it is applied in a "one-time use" or "disposal" way.

In order to fulfill all these requirements, a low-cost, high-performance tritium cell was designed at KIT which consists of a thin, custom-built light-pipe cell with an in-line tritium oxidation unit. Both elements are described in the following subsections.

2.2. Optical and mechanical design of the light-pipe cell

A sketch of the cell is presented in Fig. 2. The core of the cell is based on a hollow waveguide or light-pipe design (e.g. see [24–28]).

The infrared light is focused onto the small (about 1 mm) entrance of the cell, then internally reflected on its highly-reflective surfaces, and finally leaves the pipe carrying the absorption features of the sample gas. This geometry maximizes the product of particle density n and optical path length ℓ , which is the relevant quantity for absorption according to the Lambert-Beer-Law

$$I = I_0 \cdot e^{-\sigma n \ell} . \quad (1)$$

While the maximum particle number of radioactive material as used here is given by the legal limit, the small cross-section of the cell translates to a small volume (compared to other types of multiple reflection absorption cells), and thus higher partial pressure as compared to standard FTIR sample cells are possible with our new cell. Although the wall reflections lead to losses in the transmitted light as $R < 1$, they also lead to a small geometrical increase of the optical path length as compared to a collimated beam. It should be recalled that the objective of the light-pipe design is not to extend the path length, but to increase the particle density for same path length.

Another benefit of this cell is the simple alignment as compared to multi-reflection or cavity-enhanced techniques. In practice, the collimated IR beam is focused onto the cell entrance by a concave mirror. The entrance solid angle is generally very similar to the exit angle, and therefore the intensity of the radiation field can be coupled into the spectrometer without further losses.

One crucial part of the cell design is the selection of optical materials for the light-pipe and the coupling windows providing a high-reflectivity and transmission, respectively, in the spectral region of interest. Fig. 1 (bottom) indicates that in order to cover all bands of interest by FTIR spectroscopy, the optical quality of the materials should be high in the range of about $2500 - 10\,000$ cm^{-1} .

One of the preferred materials with high reflectivity for IR radiation (from $0.8 \mu m$ to $20 \mu m$) is polished gold. However, custom-building of highly polished gold pipes is rather complicated. But also the reflectivity R of polished aluminum in the spectral range of interest from $1 \mu m$ to $4 \mu m$ (or 2500 cm^{-1} to $10\,000$ cm^{-1}) is greater than 94 %. Aluminum pipes are available from stock with different outer diameters (OD) and inner diameters (ID) with a rather good surface quality with regard to IR reflection as obtained in the production procedure.

For the cell presented here, an aluminum pipe with OD = 6 mm and ID = 4 mm was cut to a length of 201 mm. The inner surface was further smoothed by an iterative lapping and polishing process. This pipe was fitted into off-the-shelf VCR stainless steel (face seal) fittings from Swagelok as found in fig. 2. The only VCR part which needed a custom machinery was the

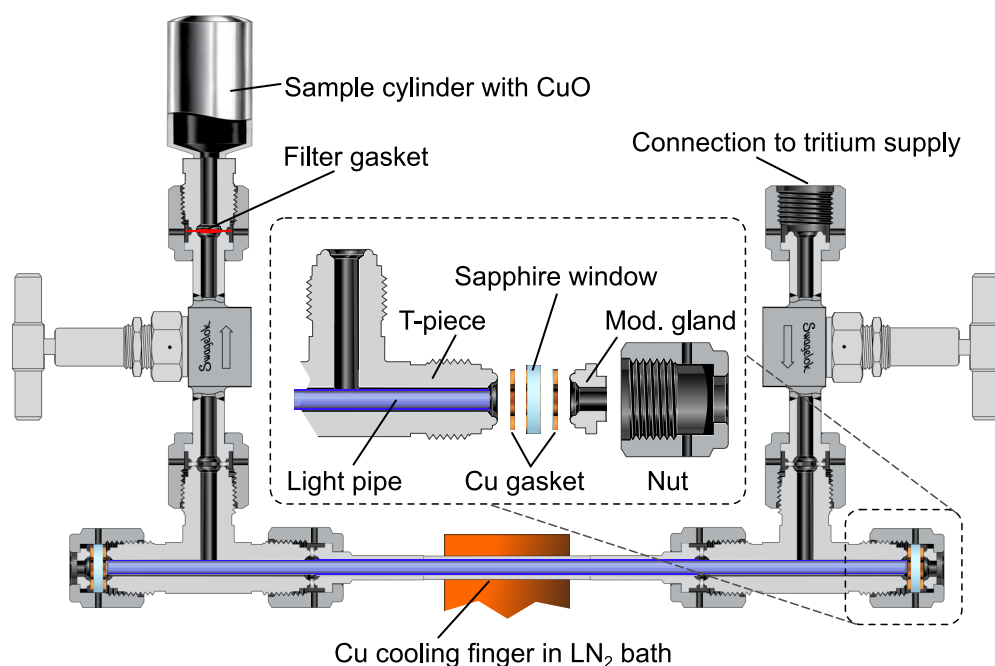


Fig. 2. Sketch of the tritium-compatible light-pipe cell. Center: Explosion sketch of the custom-built optical window sealing.

stainless steel pipe (OD = 8 mm, ID = 6 mm) with two orbitally welded VCR female fittings. Two full-metal valves enclose the gas within the cell. The aluminum pipe was further modified: a) the outer diameter was reduced using a lathe along the length of the T-piece to allow the gas flow from the valve to via the T-pieces to the light pipe entrance near the window; b) as the outer diameter of the light pipe and the inner diameter of the stainless steel tube are both 6 mm, one was inserted into the other which resulted in a snug friction fit.

Fig. 1 (bottom) also reveals, that for the range of interest, sapphire would be an ideal candidate as window material. Another essential aspect is the window-to-cell seal, as shown in the inset of fig. 2. Inspired by the work of Johnson and Eden [29], we realized the window sealing in a tight, tritium compatible, replaceable and cost-effective way. For the cell windows, a 1/2 inch wedged sapphire window (Thorlabs) was chosen offering a transmission from 2500 cm^{-1} to $12\,500\text{ cm}^{-1}$. The sealing was realized with standard Swagelok copper gaskets. We found, that for this custom construction, it is required to generate symmetric pressure on the sealing sapphire surface. Therefore, a VCR gland was modified as shown in fig. 2 and put inside the outer VCR nut which holds the sapphire window. It should be noted that only the inner gasket seals the window to the gas bearing system.

For our application the cell was tested below atmospheric pressure as there is no pressure rating on the custom copper sealed sapphire windows. We found, that the window seals' leakage rate is less than $10^{-9}\text{ mbar l s}^{-1}$ even after thermocycling the vessel between being cooled with liquid nitrogen and a bake-out at $350\text{ }^{\circ}\text{C}$.

2.3. Tritium oxidation unit

In [30] a sample of T_2O ($\sim 10\text{ Ci}$) was prepared externally and then filled into a microwave cell using a cryogenic procedure. This step requires a setup designed for tritiated water production. This kind of device, if aimed for high tritium concentrations, would need to be more elaborated,

since tritiated water with very high specific activity must be avoided in any tritium process. Earlier measurements by Carpenter et al. needed 300 Ci (approx. 11 000 GBq) of activity which was equivalent of about 120 mbar in a 58 cm long cell [31].

One option to generate tritiated water is to fill molecular tritium and oxygen gas into a closed volume and then to wait for the radiochemically induced reaction forming water. This method as performed by Fry et al. [11] appears to be simple as no special processing step appears to be necessary and both precursor gases can be directly filled into the spectroscopy cell. Kanesaka et al. used a similar method but accelerated the oxidation by using a platinum black catalyst [12]. However, filling such a cell is already a safety challenge, as the use of tritium and oxygen is generally very restricted in tritium processing due to the risk of forming explosive mixtures. Also, unreacted gas, if not removed from the reaction products, will increase the total pressure in the cell leading to line broadening and therefore fundamentally limits the maximum achievable resolution of the final spectrum.

The tritium oxidation method chosen in this work is performed similarly to Kobayashi et al. [9], using the reduction of copper(II) oxide.



Kobayashi et al. had 37 GBq available for the synthesis of tritiated water. Subsequent to the oxidation of the tritium gas, they condensed the freshly produced water in a LN₂-cooled reservoir. From this reservoir the water vapour was expanded into the spectroscopy cell. In our case, we had only 1 GBq available in order to remain below the legal limit. This 1 GBq of activity translates to $n_{\text{T}} = 9.3 \cdot 10^{-7}$ mol of tritium atoms or $pV = 22.69$ mbar cm³. Therefore, the cell volume must be minimized to achieve the highest possible pressure in the gas cell. Also, the oxidation process must ensure a conversion efficiency from tritium gas to tritiated water close to 100% without introducing contaminants or additional, undesired gas molecules. Therefore, this method needed to be optimized.

3. Performance of cell

3.1. Generation of tritiated water

Prior to the generation of tritiated water, the cell and oxidation unit were baked out to clean them from any organic contaminants and residual gases. For the bake-out, the whole assembly was placed in an oven which is constantly flushed with nitrogen to prevent oxidation of the copper seals. A turbomolecular pump was connected through a port in the oven to the cell and oxidation unit prior to the bake-out and was run continuously throughout the procedure. In a first step, the oxidation unit was heated to 350 °C using the coaxial heating cable affixed to the sample cylinder. After 4 hours, the valve connecting the cell body to the oxidation unit was closed and the coaxial heating cable was turned off, in turn the oven was switched on. The cell was baked-out for 6 hours while the pump was kept running for 4 more days until tritium gas could be filled into the gas cell.

The gas cell was filled with 1.74 mbar of molecular tritium gas (atomic composition: 97 % T, 2 % H and 1 % D). Considering the gas cell volume of 5.64 cm³, 82 % of the legally permitted amount of T₂ was transferred to the cell. All this was done in the glovebox of the TLK's tritium transfer facility. After the cell was removed from the transfer facility and the external surfaces of the cell were decontaminated, the synthesis of tritiated water could be started.

The filled gas cell was placed in a fume hood inside the TLK, where the copper cooling finger was attached to the mid-section of the cell (see fig. 2). The cooling finger was lowered into a Dewar vessel and the whole assembly was secured with a laboratory stand. Liquid nitrogen was poured into the Dewar until any boiling subsides and the oxidation unit was heated to 350 °C. Then, the valve connecting the gas cell with the oxidation unit was opened. Heating and cooling

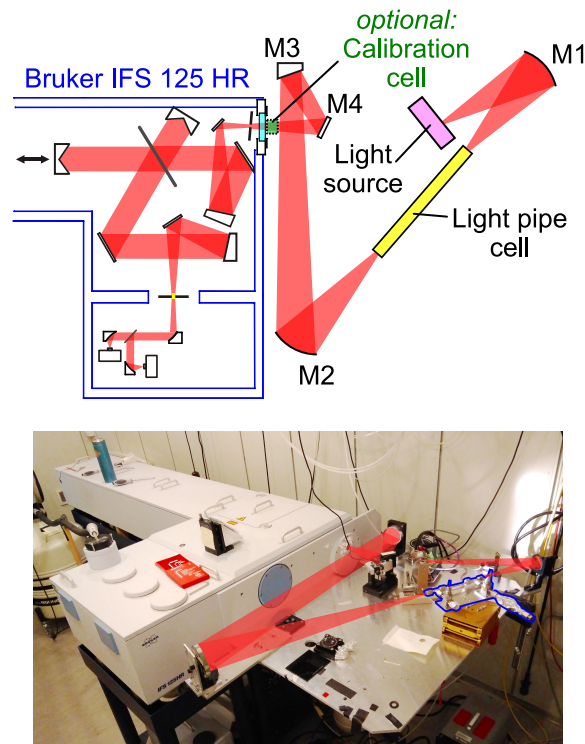


Fig. 3. (Top) Sketch of the experimental setup of the light pipe cell installed into the IMK-ASF FTIR spectrometer setup. Adapted to [35]. (Bottom) Picture of the setup (the cell is indicated in a blue contour).

was continued for 2.5 hours and liquid nitrogen was replenished when needed. After all the T_2 was oxidized, the connecting valve was closed, the heating turned off and the cooling finger detached. Now, the cell was ready for measurement; but we should also be aware of the fact that the tritiated water will decompose to hydrogen and oxygen due to the presence of ions formed by the tritium beta decay. Kobayashi et al. report, that this may amount to 5 to 10 % hydrogen/oxygen gas with regard to the water molecules [9].



It should be noted, that the pressure inside of the cell can only be determined as long it is connected to the tritium facility. After detaching and performing the combined oxidation and cryo-transport, the pressure in the interaction volume of IR light and vapor is no longer precisely known. When traces of other gases with well-known broadening parameters are present in the cell (e.g. CO_2), then the cell pressure can be estimated from the line-shape of these gases as recorded in the high-resolution FTIR spectrum.

3.2. Coupling to a high-resolution FTIR spectrometer

The spectroscopic element of the experimental setup was a Bruker IFS 125HR high-resolution FTIR spectrometer. It is generally used for atmospheric trace gas spectroscopy, but can also be illuminated by either an external halogen or a Globar light source. More details on the system and its performance can be found in [32–34].

The cell was placed on a height-adjustable lab jack. The whole beam path is shown in fig. 3.

Light from the halogen/Globar source was focused by a concave spherical gold-plated mirror M1 ($f = 150$ mm) into the center of the gas cell window. After passing through the 201 mm long cell, the light exits the cell under the same angle as the angle of incidence. The light beam is then re-focused by a second concave spherical mirror M2. The beam is further shaped and guided into the entrance port of the IFS 125HR by mirrors M3 and M4, which are an integral part of the existing setup and were left unmodified. The reproducible manual alignment of the cell into the existing optical path could be realized in less than 5 minutes, which implies that coupling this cell to any optical system is a rather straightforward task. The polished inner surfaces of the light pipe cell worked as intended since the (small) divergence of the input cone is preserved by the cell. This has been verified by checking the output light distribution from which near grazing incidence reflection can be assumed.

The transmission of infrared light through the cell was measured by comparing the free-path IR intensity to the scenario with the cell installed in the beam-path. The empirical transmission of the cell was determined to be about 20%. This result is in good qualitative agreement with the estimation when taking into account transmission and coupling losses at the windows as well as losses from multiple reflections on the polished Al surface (see fig. 1 (bottom)). The wavelength dependent transmission was found as predicted in fig. 1 (bottom) dominated by the reflectivity of aluminum. We measured a linear, relative reduction of the transmission by less than 4% at 5400 cm^{-1} with regard to 3800 cm^{-1} .

3.3. Spectroscopic performance

In a first run with the cell, a wide spectral range from 2000 to $10\,000\text{ cm}^{-1}$ was measured in about 15 h acquisition time, using $36\text{ cm } OPD_{\max}$. This value of OPD_{\max} is equivalent to a spectral resolution of 0.025 cm^{-1} (adopting the definition of resolution applied by the manufacturer of the FTIR spectrometer: $\text{resolution} = 0.9/OPD_{\max}$). The signal-to-noise ratio ranges from 60 to well over 100 which allows us to determine the center position of a typical 0.035 cm^{-1} FWHM peak in the spectrum with a precision in the order of 0.0006 cm^{-1} .

Fig. 4 shows the $2\nu_1$ band of HTO around 4500 cm^{-1} which has not been previously measured by high-resolution FTIR spectroscopy. It was selected to demonstrate the spectroscopic quality obtained with the cell in the presented hardware configuration. On the one hand, the band lays in an atmospheric transmission window meaning it is almost free of overlap with absorption features from species like H_2^{16}O . On the other hand, the $2\nu_1$ mode of HTO is not perturbed by other modes of the same molecule. The comparison to a simulated spectrum (obtained via the Toms database) with highlighted P-, Q-, R-branches shows a clear rotational structure of the semi-rigid asymmetric top rotor. The complete experimental line list and the derivation of molecular constants will be published in a separate publication. In the entire recorded spectrum, we find further modes of HTO, which are less isolated than the one presented in fig. 4, like the $2\nu_2$ mode which was recently published [36].

The structure on the baseline in the spectrum in fig. 4 is due to minor etaloning. This is an effect from the combination of numerous optical resonators present in the beam path of such a complex setup (entrance windows of detector, optical filters, tungsten lamp bulb, beam splitter, cell windows, etc).

A fit of the line intensities of HTO and T_2O combined with the theoretical intensities by Partridge and Schwenke [1] gives the ratio of those isotopologues. This calculation yields 91.3% HTO and 8.7% T_2O present in the gas cell, not taking light water species into account as H_2O lines are overlapped by atmospheric lines.

4. Conclusion

Accurate spectroscopic data sets of tritiated water molecules are very interesting for benchmarking quantum theoretical models. However, the fact that these molecules are radioactive and thus

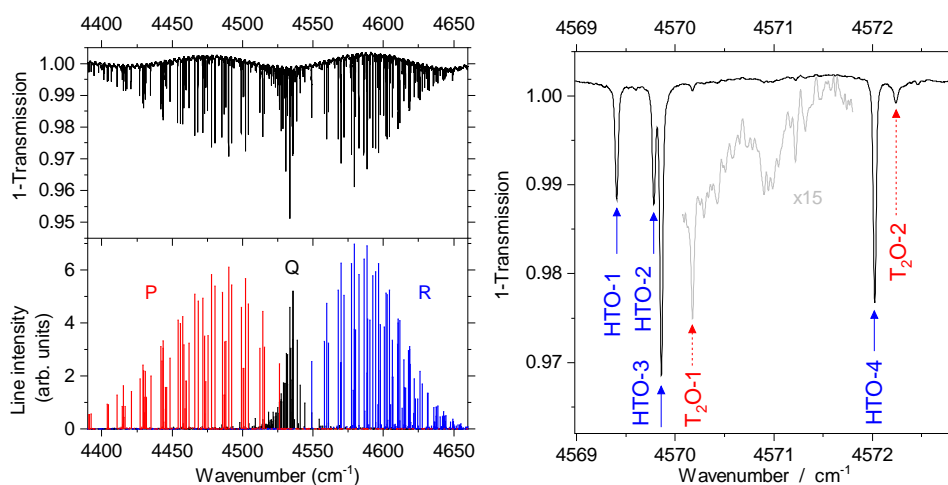


Fig. 4. (Top left): The experimentally measured $2\nu_1$ band of HTO. (Bottom left) Simulated spectrum by utilizing data from the Tomsk variational calculation database. (Right) Zoomed in section. The individual lines are assigned according to calculations by Partridge and Schwenke as tabulated in table 1.

Table 1. Line Assignment, According to Partridge [1] taken from the Tomsk Database (Corrected for Natural Abundance).

Line	ν cm^{-1}	I_{meas} $\text{cm}/\text{molecule}$	Branch	J'	K'_a	K'_c	J''	K''_a	K''_c
T ₂ O-1	4570.18	$5.27 \cdot 10^{-22}$	$\nu_1 + \nu_3$	3	1	2	2	1	1
T ₂ O-2	4572.25	$6.69 \cdot 10^{-22}$	$\nu_1 + \nu_3$	4	1	4	3	1	3
HTO-1	4569.41	$5.04 \cdot 10^{-22}$	$2\nu_1$	3	0	3	2	0	2
HTO-2	4569.78	$5.03 \cdot 10^{-22}$	$2\nu_1$	3	1	2	2	1	1
HTO-3	4569.86	$1.26 \cdot 10^{-21}$	$2\nu_1$	3	2	2	2	2	1
HTO-4	4572.03	$1.01 \cdot 10^{-21}$	$2\nu_1$	3	2	1	2	2	0

pose experimental challenges, make such data very scarce. We plan to resolve this deficit by broadband FTIR studies of various tritiated water isotopologues (including ^{17}O , ^{18}O) for which we have developed a dedicated absorption cell. Here we have demonstrated that the fully tritium-compatible, custom-built light-pipe cell was successfully coupled to a high-resolution FTIR spectrometer. By making use of the internal reflection of the cell by design, we were able to amplify also weak absorption lines in order to achieve a signal-to-noise ratio sufficiently strong for high-resolution spectroscopy. The spectroscopic power of the technique was demonstrated on the $2\nu_1$ branch of HTO. That showed that it is suitable for the spectroscopic investigation of the molecular structure of radioactive molecules in a wide spectral range. For time-critical trace detection applications dedicated laser spectroscopy (especially with cavity enhancement) will provide superior sensitivity. The in-situ production of the radioactive sample in the cell proved to be very efficient in reducing waste and limiting safety risks. It should be emphasized that the cost for such a cell is rather low, which is indeed very cost-efficient as compared to other

multi-reflection or cavity-enhanced cell types. We suggest that this type of cell is also suitable for spectroscopy of other tritiated gas (e.g. CT₄, NT₃) or even other hazardous molecular gases which are generated externally, or in the cell, as demonstrated here.

Acknowledgments

We thank Tobias Falke, Tobias Weber and Stefan Welte for the support in designing, producing and testing of the copper-to-glass sealing and the entire cell.

References

1. H. Partridge and D. W. Schwenke, "The determination of an accurate isotope dependent potential energy surface for water from extensive ab initio calculations and experimental data," *J. Chem. Phys.* **106**, 4618–4639 (1997).
2. N. F. Zobov, O. L. Polyansky, C. L. Sauer, and J. Tennyson, "Vibration-rotation levels of water beyond the Born-Oppenheimer approximation," *Chem. Phys. Lett.* **260**, 381–387 (1996).
3. O. L. Polyansky, R. I. Ovsyannikov, A. A. Kyuberis, L. Lodi, J. Tennyson, and N. F. Zobov, "Calculation of rotation-vibration energy levels of the water molecule with near-experimental accuracy based on an ab initio potential energy surface," *J. Phys. Chem. A* **117**, 9633–9643 (2013).
4. G. P. Kincaid Jun and E. R. Ibert, "Tritium production from nitrogen in fission reactors," *Nature* **226**, 139 (1970).
5. J. S. Watson, C. E. Easterly, J. B. Cannon, and J. B. Talbot, "Environmental effects of fusion power plants. part ii: Tritium effluents," *Fusion Technol.* **12**, 354–363 (1987).
6. M. B. Kalinowski, "Uncertainty and range of alternatives in estimating tritium emissions from proposed fusion power reactors and their radiological impact," *J. Fusion Energ.* **12**, 157–161 (1993).
7. M. Velarde, L. Sedano, and J. Perlado, "Dosimetric impact evaluation of primary coolant chemistry of the internal tritium breeding cycle of a fusion reactor DEMO," *Fusion Sci. Technol.* **54**, 122–126 (2008).
8. P. P. Cherrier and J. Reid, "High-sensitivity detection of tritiated water vapour using tunable diode lasers," *Nucl. Instrum. Meth. A* **257**, 412–416 (1987).
9. K. Kobayashi, T. Enokida, D. Iio, Y. Yamada, M. Hara, and Y. Hatano, "Near-infrared spectroscopy of tritiated water," *Fusion Sci. Technol.* **60**, 941–943 (2011).
10. C. Bray, A. Pailloux, and S. Plumeri, "Tritiated water detection in the 2.17 μm spectral region by cavity ring down spectroscopy," *Nucl. Instrum. Meth. A* **789**, 43–49 (2015).
11. H. Fry, L. Jones, and J. Barefield, "Observation and analysis of fundamental bending mode of T₂O," *J. Mol. Spectrosc.* **103**, 41–55 (1984).
12. I. Kanesaka, M. Tsuchida, K. Kawai, and T. Takeuchi, "The IR spectrum of T₂¹⁸O," *J. Mol. Spectrosc.* **104**, 405–413 (1984).
13. S. Cope, D. Russell, H. Fry, L. Jones, and J. Barefield, "Analysis of the fundamental asymmetric stretching mode of T₂O," *J. Mol. Spectrosc.* **120**, 311–316 (1986).
14. S. Cope, D. Russell, H. Fry, L. Jones, and J. Barefield, "Analysis of the ν_1 fundamental mode of HTO," *J. Mol. Spectrosc.* **127**, 464–471 (1988).
15. O. Ulenikov, V. Cherepanov, and A. Malikova, "On analysis of the ν_2 band of the HTO molecule," *J. Mol. Spectrosc.* **146**, 97–103 (1991).
16. A. Fayt and G. Steenbeckeliers, "Determination of the ν_1 and ν_3 vibrational levels of the radioactive water molecule HTO by high resolution infrared spectroscopy and calculation of rotation constants of the fundamental state," *C. R. Acad. Sci. Paris Ser. B* **275**, 459–460 (1972).
17. M. J. Down, J. Tennyson, M. Hara, Y. Hatano, and K. Kobayashi, "Analysis of a tritium enhanced water spectrum between 7200 and 7245 cm^{-1} using new variational calculations," *J. Mol. Spectrosc.* **289**, 35–40 (2013).
18. A. D. Rakić, "Algorithm for the determination of intrinsic optical constants of metal films: application to aluminum," *Appl. Opt.* **34**, 4755–4767 (1995).
19. P. B. Johnson and R. W. Christy, "Optical constants of the noble metals," *Phys. Rev. B* **6**, 4370–4379 (1972).
20. P. Souers, *Hydrogen Properties for Fusion Energy* (University of California Press, 1986).
21. D. MacMahon, "Half-life evaluations for ³H, ⁹⁰Sr, and ⁹⁰Y," *Appl. Radiat. Isot.* **64**, 1417–1419 (2006).
22. J. Orphal and A. A. Ruth, "High-resolution fourier-transform cavity-enhanced absorption spectroscopy in the near-infrared using an incoherent broad-band light source," *Opt. Express* **16**, 19232–19243 (2008).
23. S. Chandran and R. Varma, "Near infrared cavity enhanced absorption spectra of atmospherically relevant ether-1, 4-dioxane," *Spectrochim. Acta A* **153**, 704–708 (2016).
24. M. Yin, B.-Z. Yu, and W. N. Hansen, "The optical design and application of light pipe systems in FTIR spectrometer," *Proc. SPIE* **1145**, 451–452 (1989).
25. P. Yang, E. L. Ethridge, J. L. Lane, and P. R. Griffiths, "Optimization of GC/FT-IR measurements i: Construction of light-pipes," *Appl. Spectrosc.* **38**, 813–816 (1984).
26. P. W. J. Yang and P. R. Griffiths, "Optimization of GC/FT-IR measurements ii: Optical design," *Appl. Spectrosc.* **38**, 816–821 (1984).
27. D. F. Gurka and S. M. Pyle, "Qualitative and quantitative environmental analysis by capillary column gas chromatography/lightpipe Fourier-transform infrared spectrometry," *Environ. Sci. & Technol.* **22**, 963–967 (1988).

28. H. Malissa, "On the use of capillary separation columns in GC/FTIR-spectroscopy and on the quantitative evaluation of the Gram-Schmidt reconstructed chromatogram," *Fresen. Z. Anal. Chem.* **316**, 699–704 (1983).
29. D. E. Johnson and J. G. Eden, "High-temperature, alkali-rare gas optical cell," *Rev. Sci. Instrum.* **57**, 2976–2978 (1986).
30. F. C. De Lucia, P. Helminger, W. Gordy, H. W. Morgan, and P. A. Staats, "Millimeter- and submillimeter-wavelength spectrum and molecular constants of T₂O," *Phys. Rev. A* **8**, 2785–2791 (1973).
31. R. A. Carpenter, N. M. Gailar, H. W. Morgan, and P. A. Staats, "The ν_2 fundamental vibration-rotation band of T₂O," *J. Mol. Spectrosc.* **44**, 197–205 (1972).
32. F. Hase, "Improved instrumental line shape monitoring for the ground-based, high-resolution FTIR spectrometers of the Network for the Detection of Atmospheric Composition Change," *Atmos. Meas. Tech.* **5**, 603–610 (2012).
33. F. Hase, B. J. Drouin, C. M. Roehl, G. C. Toon, P. O. Wennberg, D. Wunch, T. Blumenstock, F. Desmet, D. G. Feist, P. Heikkinen, M. De Mazière, M. Rettinger, J. Robinson, M. Schneider, V. Sherlock, R. Sussmann, Y. Té, T. Warneke, and C. Weinzierl, "Calibration of sealed HCl cells used for TCCON instrumental line shape monitoring," *Atmos. Meas. Tech.* **6**, 3527–3537 (2013).
34. M. Kiel, F. Hase, T. Blumenstock, and O. Kirner, "Comparison of XCO abundances from the Total Carbon Column Observing Network and the Network for the Detection of Atmospheric Composition Change measured in Karlsruhe," *Atmos. Meas. Tech.* **9**, 2223–2239 (2016).
35. M. Gisi, F. Hase, S. Dohe, and T. Blumenstock, "Camtracker: a new camera controlled high precision solar tracker system for FTIR-spectrometers," *Atmos. Meas. Tech.* **4**, 47–54 (2011).
36. J. Reinking, M. Schlösser, F. Hase, and J. Orphal, "First high-resolution spectrum and line-by-line analysis of the $2\nu_2$ band of HTO around 3.8 microns," *J. Quant. Spectrosc. Ra.* **230**, 61–64 (2019).